

We are IntechOpen, the world's leading publisher of Open Access books Built by scientists, for scientists

6,900

Open access books available

186,000

International authors and editors

200M

Downloads

Our authors are among the

154

Countries delivered to

TOP 1%

most cited scientists

12.2%

Contributors from top 500 universities



WEB OF SCIENCE™

Selection of our books indexed in the Book Citation Index
in Web of Science™ Core Collection (BKCI)

Interested in publishing with us?
Contact book.department@intechopen.com

Numbers displayed above are based on latest data collected.
For more information visit www.intechopen.com



Analysis of Long-Periodic Fluctuations of Solar Microwave Radiation, as a Way for Diagnostics of Coronal Magnetic Loops Dynamics

Maxim L. Khodachenko¹, Albert G. Kislyakov² and Eugeny I. Shkelev²

¹*Space Research Institute, Austrian Academy of Sciences, Graz,*

²*Lobachevsky State University, Nizhny Novgorod,*

¹*Austria*

²*Russia*

1. Introduction

The solar corona has a very complex and highly dynamic structure. It consists of a large number of constantly evolving, loops and filaments, which interact with each other and are closely associated with the local magnetic field. The non-stationary character of solar plasma-magnetic structures manifests itself in various forms of the coronal magnetic loops dynamics as rising motions, oscillations, meandering, twisting (Aschwanden et al., 1999; Schrijver et al., 1999), as well as in formation, sudden activation and eruption of filaments and prominences. Energetic phenomena, related to these types of magnetic activity, range from tiny transient brightenings (micro-flares) and jets to large, active-region-sized flares and coronal mass ejections (CMEs). They are naturally accompanied by different kinds of electromagnetic (EM) emission, covering a wide frequency band from radio waves to gamma-rays. Radiation, produced within a given plasma environment, carries an information on physical and dynamic conditions in a radiating source. This causes an exceptional importance of the EM radiation, as a diagnostic tool, for understanding the nature and physics of various solar dynamic phenomena. As a relatively new, in that context, direction of study in the traditional branch of the solar microwave radio astronomy appears the analysis of the slow, long-periodic (e.g., > 1 s) fluctuations of the radiation intensity (Khodachenko et al., 2005; Zaitsev et al., 2003).

Microwave radiation from the magnetic loops in solar active regions (e.g., during solar flares) is usually interpreted as a gyro-synchrotron radiation, produced by fast electrons on harmonics of the gyro-frequency ν_B in the magnetic field B of the loop. In the case of a power-law distribution of electrons in energy as $f(\mathcal{E}) \propto \mathcal{E}^{-\delta}$, the intensity of gyro-synchrotron radiation I_ν from an optically thin loop (Dulk, 1985; Dulk & Marsh, 1982) is

$$I_\nu \propto B^{-0.22+0.9\delta} (\sin \theta)^{-0.43+0.65\delta}, \quad (1)$$

where θ is the angle between magnetic field and the direction of electromagnetic wave propagation. For the observed typical values of the electron energy spectrum index $2 \leq \delta \leq 7$ this implies the proportionality of intensity to a moderately high power of the background

magnetic field and essential anisotropy of the radiation: $I_\nu \propto B^{1.58 \div 6.08} (\sin \theta)^{0.87 \div 4.12}$. Equation (1) is obtained within an assumption of an optically thin source, when the radiation intensity is proportional to the emissivity η_ν (Dulk, 1985). According to the estimations in Urpo et al. (1994), a coronal loop with diameter of about 4×10^8 cm is optically thin in the considered frequency range for the gyro-synchrotron absorption if the density of fast electrons is $< 2 \times 10^9$ cm⁻³. The typical density of > 10 keV electrons in the microwave burst events is usually $10^6 \div 10^7$ cm⁻³ and therefore, it stays well within the above indicated limit.

It follows from the equation (1) that variations of the loop magnetic field, associated with disturbances of the electric current in a radiating source, should modulate the intensity of the microwave radiation of the loop (Khodachenko et al., 2005; Zaitsev et al., 2003). Another origin for the modulation of intensity of the observed microwave radiation can be due to the quasi-periodic motion (oscillation) of a coronal magnetic loop, containing the radiation source. This mechanism is connected with the anisotropy of the gyro-synchrotron emission, as well as with the variation of the magnetic field value during the oscillatory motion of the loop, which both, according to the equation (1), can result in a quasi-periodic modulation of the received signal (Khodachenko et al., 2006; 2011). Therefore, the analysis of slow modulations of solar microwave radiation may be used for the diagnostics of oscillating electric currents in the coronal loops, as well as for the investigation of large-scale motion of the loops (including loop oscillations) in solar active regions. By this, it is natural to expect that structural complexity of solar active regions will manifest itself in peculiarities of the emitted radiation.

The dynamic spectra of the long-periodic oscillations, modulating the intensity of microwave radiation from solar active regions, have been found to contain quite often several spectral tracks, demonstrating a specific temporal behaviour (Zaitsev et al., 1998; 2001a;b; 2003). Khodachenko et al. (2005) considered these multi-track features as an indication that the detected microwave radiation is produced within a system of a few closely located, magnetic loops, having slightly different parameters and involved in a kind of common global dynamic process. In several cases such slow modulations of solar microwave radiation (with multi-track spectra) were interpreted as the signatures of oscillating electric currents, running within the circuits of moving relative each other inductively connected coronal magnetic loops (Khodachenko et al., 2006). The dynamics of these electric currents has been described by means of the equivalent electric circuit (LCR-circuit) models of the coronal loops (Khodachenko et al., 2003; Zaitsev et al., 1998) characterized by time-dependent inductance L , capacitance C , resistance R , as well as mutual inductance coefficients M_j (Khodachenko et al., 2003; 2009). The L , C , R and M_j parameters of electric circuit of a current-carrying loop depend on shape, scale, position of the loop with respect to other loops, as well as on the plasma parameters and value of the total longitudinal current in the magnetic tube. In that respect it is worth to mention that the LCR-circuit model ignores the fact that changes of the magnetic field and related electric current propagate in plasma at the Alfvén speed. It ignores any short-time variations of plasma parameters, which appear to be averaged in course of derivation of the LCR model equation (Khodachenko et al., 2009; Zaitsev et al., 2001a). The LCR approach assumes instant changes of the electric current over the whole electric circuit according to the varying potential and ignores all the "propagation effects" related to the system MHD modes. The LCR equations correctly describe temporal evolution of electric currents in a system of solar magnetic current-carrying loops only at a time scale longer than the Alfvén wave propagation time. More generally, the equivalent electric circuit model of a coronal loop tends to emphasize the global electric circuit, obscuring the effects of the

ambient plasma and details of the magnetic structure. The LCR model approach was applied in particular for interpretation of the solar microwave burst long-periodic modulations with drifting modulation frequencies $\nu(t)$ in the interval $0.03 \div 1$ Hz. Based on the analysis of the frequency drift of the modulations Zaitsev et al. (1998; 2001a; 2003) and Khodachenko et al. (2005) estimated also the values of the electric current in flaring loops ($10^8 \div 10^{11}$ A), which appeared to be close to the values obtained by other methods (Hardy et al., 1998; Leka et al., 1996; Moreton & Severny, 1968; Spangler, 2007; Tan et al., 2006).

However, not all long-periodic modulations of solar microwave radiation demonstrate frequency drift and occupy a similar frequency range. Khodachenko et al. (2009) pointed out that the frequency of LCR-oscillations of the electric current, which depends on specific parameters of a coronal loop, usually stays within the interval $\nu_{LCR} \approx (0.03 \div 1)$ Hz. Therefore, the modulations of the solar microwave radiation intensity with $0.03\text{Hz} < \nu < 1\text{Hz}$ are very likely to be due to the electric currents, oscillating in LCR-circuits of coronal loops. At the same time, modulations caused by the oscillatory motions of loops that contain the radiation sources, because of their direct connection with the large-scale dynamics of loops, should have typical frequencies < 0.01 Hz and exhibit no drift. Thus, it has been proposed in (Khodachenko et al., 2009) that one should distinguish, when speaking about different kinds of long-periodic modulations of the solar microwave radiation, between the *low-frequency (LF)* ($\approx 0.03 \div 1$ Hz) and *very-low-frequency (VLF)* (< 0.01 Hz) modulations, assuming the first to be connected with the LCR-oscillations of electric currents in the coronal loops and the second to be caused by large-scale motions of the radiation sources confined within the oscillating loops. LF modulations (e.g., $0.03 \div 1$ Hz) have been studied in details and interpreted in terms of the equivalent electric circuit models of coronal loops in Khodachenko et al. (2005; 2006); Zaitsev et al. (1998; 2001a;b; 2003). They are not considered in this chapter, whereas we address here the VLF modulations (< 0.01 Hz) of solar microwave radiation and their possible relation to the large-scale dynamics of coronal loops in solar active regions. Some preliminary results on that subject were reported recently in a short publication Khodachenko et al. (2011), and the present paper addresses this topic in more details.

Transverse oscillations of the coronal magnetic loops considered here are triggered by flares and filament eruptions, i.e. by phenomena in which the significant Lorentz forces are likely acting in association with the magnetic field adjustments. By this, all considered oscillating loops have at least one footpoint in the immediate vicinity of a separatrix surface or of a flare ribbon. Using the potential-field extrapolations Schrijver & Brown (2000) demonstrated that the field lines close to a separatrix surface exhibit strongly amplified displacements in response to small displacements in the photospheric "roots". This means that the magnetic field lines in the proximity of separatrix are much more sensitive to changes in the field sources than are the field lines that lie well within domains of connectivity. Speaking about a nature of the observed transversal oscillations of coronal loops Schrijver et al. (2002) address two models: (a) transverse waves in coronal loops that act as wave guides and (b) mentioned above, strong sensitivity of the shape of magnetic field lines near separatrix to changes in the bottom field sources. By this, the authors outline several observational features that favor the model (b). Based on the extensive study of properties of transverse loop oscillations triggered by flares, Aschwanden et al. (2002) also concluded that most of the loops do not fit the simple model of a kink eigen-mode oscillation. Therefore, the present paper is not dedicated to the study of MHD oscillations in solar coronal loops. Our goal consists in demonstration of the fact that quasi-periodic transverse motions of a coronal magnetic loop, which contains

a source of microwave emission, may be connected with a specific modulation of radiation intensity received by a remote observer.

Speaking about other possible mechanisms (besides of the microwave radiation source large-scale oscillatory motion), which may cause a quasi-periodic modulation of the non-thermal electron gyro-synchrotron radiation, it is necessary to mention that a quasi-periodically varying flow of the non-thermal electrons may also result in oscillations of intensity of microwave radiation. Generation of energetic electrons usually is believed to be associated with the processes of magnetic reconnection during solar flares (Miller et al., 1997). There are also theories which suggest acceleration of particles by the inductive and charge separation electric fields, build in course of the continuous motion of solar large-scale coronal magnetic structures (Khodachenko et al., 2003; Zaitsev & Stepanov, 1992). Besides of that, particle acceleration in a collapsing magnetic trap (Karlický & Kosugi, 2004), in the MHD turbulence (LaRosa & Moore, 1993; Miller et al., 1996), and in shocks (Cargill et al., 1988; Holman & Pesses, 1983) are addressed as secondary possible mechanisms for energetic particle production. An extended review of particle acceleration processes in solar flares was recently published by Aschwanden (2002). In most of these cases the typical periods are shorter than those of the VLF transverse oscillations of coronal loops. On the other hand, there are also models in which VLF large-scale oscillations of coronal loops control the process of generation of energetic particles after the impulsive phase of a flare (Nakariakov et al., 2006). This case, however, deserves a special study, which appears beyond the scope of the present paper. Our analysis here is based on the traditional scenario, according to which the non-thermal particles, produced during a flare in particle acceleration regions (e.g., sites of magnetic reconnection or the area of separatrix currents), are injected into oscillating loops.

2. Peculiarities of VLF modulations of microwave radiation related to large-scale transverse motions of the radiating sources in the oscillating coronal loops

Even taking into account the typical ranges of the modulation frequencies of microwave radiation (mentioned above), it is usually difficult to identify the modulation mechanism acting in each particular case. Indeed, having in mind only Equation (1) one cannot say for sure if the observed modulation is due to *a*) the electric current oscillations in the radiation source or *b*) the large-scale oscillatory motion of the loop. However, regarding the last modulation mechanism, an attention should be paid to the fact that large-scale transverse oscillatory motion of a coronal loop is accompanied by the periodic stress of magnetic field created in the loop, especially near its footpoints, during each inclination, i.e. two times per oscillation cycle. This means that the magnetic field strength fluctuates during the oscillatory motion of the loop with a half-period $P_{\text{osc}}/2$ of the loop oscillation. Therefore, according to Equation (1), for a transverse oscillating loop, a properly located observer, in addition to the modulation caused by the emission diagram motion at the main oscillation frequency $\nu_0 = 1/P_{\text{osc}}$, may see in some cases the modulation at the double frequency of the loop oscillation $2\nu_0$, as well as weak higher order harmonics caused by the non-linearity of Equation (1). However, as it will be shown below the relative amplitude of the higher-order harmonics, i.e., with numbers > 2 is rather low, and in the most cases only the first two harmonic frequencies can be detected. The domination of the main and double-frequency harmonics in the spectrum is caused by implicit presence of these frequencies in the signal, according to the above described character of the radiation modulating factors. Therefore, the presence of the "modulation pairs" in the low-frequency spectra, i.e., the lines which can

be associated with the main and double frequency of the loop oscillation (ν_0 and $2\nu_0$) may indicate about a transverse oscillatory dynamics of the loop.

Formation of the "modulation pairs" and their higher-order harmonic companions in multi-line dynamic spectrum of the VLF modulation of microwave radiation emitted from a transverse oscillating coronal loop may be illustrated with a simple model. Let's suppose that the loop undergoes oscillations in the direction transverse to the loop plane as shown in Figure 1. The loop inclination relative to the vertical direction varies as $\alpha(t) = \alpha_0 \sin(2\pi\nu_0 t)$, where α_0 and ν_0 are the angular amplitude and frequency of the loop oscillations, respectively. Assuming that this loop, when oriented vertically, is seen by a remote observer at the angle Θ_0 , we get that in course of the loop oscillation the viewing angle changes as $\Theta(t) = \Theta_0 - \alpha(t)$.

Irrespective of the nature of a coronal loop oscillation, the important feature of the large-scale transverse motion of the loop, consists in an oscillating magnetic stress, created in the loop during its quasi-periodic inclinations. Assuming the local transverse disturbance of the magnetic field relative its initial vertical direction to be δB , we find that the total disturbed magnetic field is $\delta B / \cos \alpha(t)$. For sufficiently small $\alpha(t)$ the following approximation can be used: $1/(\cos \alpha(t)) \approx 1/(1 - \alpha(t)^2)^{1/2} \approx 1 + (1/2)\alpha(t)^2$. This means that the disturbed magnetic field in the loop varies in time as $B(t) \approx \delta B(1 + (1/2)\alpha(t)^2)$. Therefore, for the assumed above sinusoidal character of $\alpha(t)$, we finally obtain that the local magnetic field in a transverse oscillating magnetic loop may be approximated as $B(t) \propto (1 + 0.5\alpha_0^2 \sin^2(2\pi\nu_0 t))$. Substitution of the expressions for $\Theta(t)$ and $B(t)$ into (1) enables to construct a modeling signal for the varying intensity of microwave radiation emitted from a transverse oscillating magnetic loop. The examples of dynamic spectra of this signal obtained with $\alpha_0 = \pi/6$ and $\delta = 5$ for different viewing angles $\Theta_0 = \pi/2; \pi/3; \pi/4; \pi/6$ are shown in Figure 2.

Dynamical spectra of the modeling signal in Figure 2 demonstrate several important features, typical for the radiation emitted from a microwave source located in a transverse large-scale oscillating magnetic loop, which may be observed in the solar microwave emission. In particular, for the most of the viewing angles (except of $\Theta_0 = \pi/2$) the dynamic spectra contain well pronounced "modulation pairs", e.g. the lines at the main ν_0 and double $2\nu_0$ frequency of the oscillation. Besides of that, sometimes also a weak third harmonic at $3\nu_0$ may be observed, which appears due to essentially non-sinusoidal (non-harmonic) character of the signal resulted from the joint action of two modulating factors: quasi-periodic magnetic stress and emission diagram motion. In a special case of $\Theta_0 = \pi/2$, the absence of the main frequency component is caused by a "symmetrizing" (in this case) of the varying angular part of the emission intensity. This results in a situation when the diagram motion and magnetic stress factors work synchronously.

As it can be seen in Figure 2, only the first two harmonics have high enough amplitudes. In particular, the spectral amplitude of third harmonic in the cases with $\Theta_0 = \pi/3; \pi/4; \pi/6$, never exceeds 25% of the main frequency component, whereas the second harmonic constitutes usually about 65% of the last. Therefore, the detection of harmonics with numbers higher than 2 in a natural signal, will be in the most cases difficult due to the noise contamination. The presence of modulation pairs in the VLF spectra of solar microwave radiation may be considered as an imprint of a transverse kink-type motion of a loop containing the radiation source. This feature may be used for the indirect identification of candidates for transverse oscillating coronal loops by finding specific modulation lines in the VLF dynamic spectra of microwave radiation. However, the exact detection of transverse

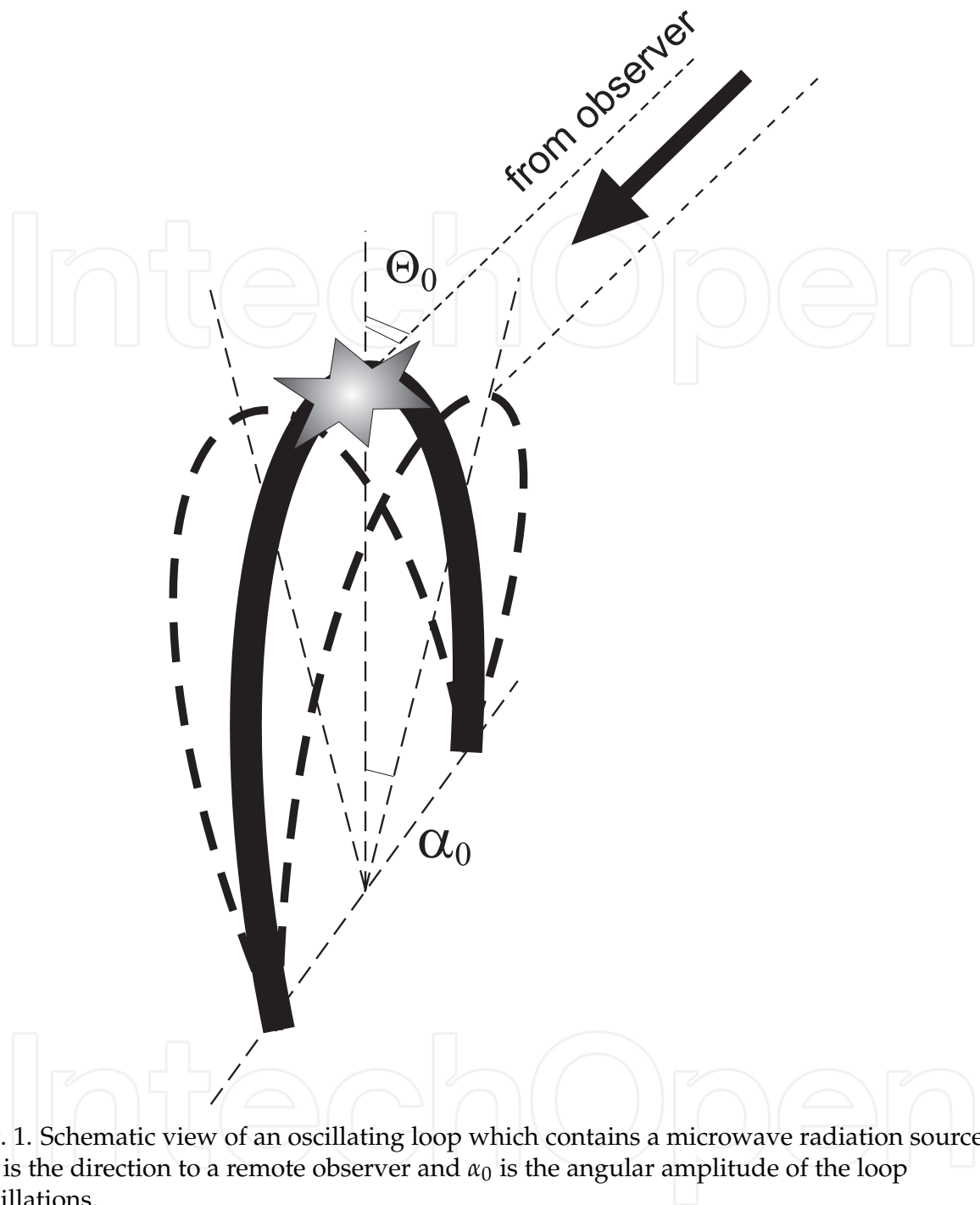


Fig. 1. Schematic view of an oscillating loop which contains a microwave radiation source. Θ_0 is the direction to a remote observer and α_0 is the angular amplitude of the loop oscillations.

motion of the radiating loops by the dynamical spectra of microwave emission (with the exclusion of other mechanisms which may also generate higher spectral harmonics) requires quantitative study of the measured radio signal and superimposing these results with the precise calculation of the radiation from the loop, taking into account the loop position relative observer.

Several real observational examples are considered below, for which VLF modulations of microwave radiation could be associated with the observed in EUV post-flare oscillating coronal loops.

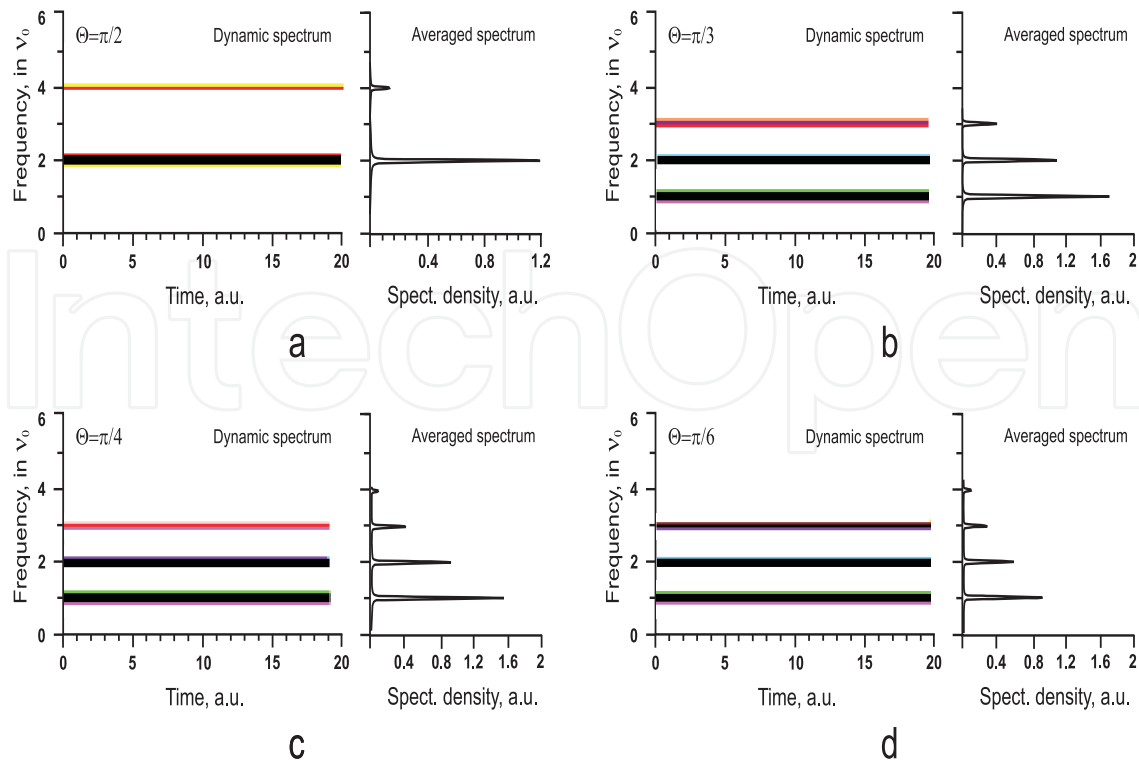


Fig. 2. Dynamical spectra of the modeling signal with $\alpha_0 = \pi/6$ and $\delta = 5$ demonstrating the peculiarities of the microwave radiation VLF modulations produced due to large-scale transverse oscillations of a coronal loop containing the radiating source. Different directions to an observer Θ_0 (viewing angles) are considered: (a) $\pi/2$; (b) $\pi/3$; (c) $\pi/4$; (d) $\pi/6$.

3. Data preparation and analysis methods

Differently to the idealized infinite in time analytical modelling signal considered in section 2, the natural radio emission received from a solar active region with oscillating coronal loop(s) is essentially time-dependent. It usually begins with an impulsive phase of a solar flare and has duration of only several periods of decaying oscillations of the loop(s). Besides of that, a signal from a particular oscillating loop is quite often strongly contaminated by interfering signals from neighboring loops in the active region of interest, as well as by the radiations emitted from other solar active regions. This complicates the task of detection and diagnostics of coronal magnetic loop oscillations in microwaves and requires special data preparation procedures with consequent application of high spectral and time resolution data analysis techniques.

Since the analyzed data appear in a form of discrete counts of the signal intensity, it is natural that digital methods are applied for their processing. A basic specifics of the digital methods consists in certain limitation of dynamical range of the resulting spectra which may lead to the loss of relatively weak and short-time, but important parts of the whole spectra-temporal picture of the studied phenomenon. To avoid of that, the analyzed data pass certain pre-processing preparation which (depending on particular case and task) may include the following procedures: 1) Subtraction of a constant component of a signal, or the signal average; 2) subtraction of a slow (as compared to the analyzed oscillations) major trend of the signal; 3) slow polynomial approximation of the analyzed data with the consequent subtraction of the approximating signal; 4) signal "normalization" (will be described below);

and 5) digital filtration of contaminating components. Altogether, the "subtraction" methods 1-3 enhance visibility of weaker fluctuations of the radiation, enabling better analysis of their spectral and temporal characteristics. Note, that the digital filtration (e.g., the method 5) with an appropriate filter(s) may efficiently substitute all the "subtraction" methods. However, the inertness of a filter results in some smoothing of the radio emission fluctuations of interest. Besides of that, information about the intensity of the radiation fluctuations is lost during the frequency filtration.

The filtration algorithm consists in the application of a Gaussian window to the analyzed signal spectrum, obtained with the discrete Fourier transform (DFT), with the consequent performance of the reverse DFT. The Gaussian window for the low frequency (LF), high frequency (HF), band-pass (BP), and band-lock (BL) filters, respectively, is determined by the following expressions:

$$\begin{aligned} W_{LF}(k) &= \exp \left\{ -\frac{k^2}{2} \cdot \left(\frac{f_1}{f_s} \cdot d \cdot N \right)^{-2} \right\}, & k = 0, \dots, N/2; \\ W_{HF}(k) &= 1 - \exp \left\{ -\frac{k^2}{2} \cdot \left(\frac{f_1}{f_s} \cdot d \cdot N \right)^{-2} \right\}, & k = 0, \dots, N/2; \\ W_{BP}(k) &= \exp \left\{ -\frac{1}{2} \cdot \left(\frac{k}{N} - \frac{f_0}{f_s} \right)^2 \cdot \left(\frac{\Delta f}{f_s} \cdot d \right)^{-2} \right\}, & k = 0, \dots, N/2; \\ W_{BL}(k) &= 1 - \exp \left\{ -\frac{1}{2} \cdot \left(\frac{k}{N} - \frac{f_0}{f_s} \right)^2 \cdot \left(\frac{\Delta f}{f_s} \cdot d \right)^{-2} \right\}, & k = 0, \dots, N/2. \end{aligned} \quad (2)$$

Here N is the number of counts in the analyzed signal, f_s is the frequency of discretization, d is decimation coefficient (Marple, 1986), f_1 is the cut-off frequency for the LF and HF filters, f_0 and Δf , are the central frequency and the band, respectively, for the BP and BL filters.

Let's consider now the "normalization" method. It is based on a treatment of an analytical signal $z(n)$ (Marple, 1986):

$$z(n) = s(n) + is_H(n) = M(n) \exp(i\Psi(n)), \quad (3)$$

where $s(n)$ and $s_H(n)$ are the analyzed digital signal and its Hilbert conjugate, respectively, and n is the count number. The parameters $M(n)$ and $\Psi(n)$ are the module and phase of the analytical signal, which are defined as the following:

$$\begin{aligned} M(n) &= \sqrt{s(n)^2 + s_H(n)^2}, \\ \Psi(n) &= \arctan \left[\frac{s_H(n)}{s(n)} \right]. \end{aligned} \quad (4)$$

The "normalization" procedure consists in division of the analytical signal $z(n)$ on $M(n)$. By this, the amplitudes of all spectral components of the analyzed process $s(n)$ become to be equalized. Note, that due to the orthogonality of functions $s(n)$ and $s_H(n)$, the value of function $M(n)$ never becomes zero. The "normalization" method is especially efficient for the analysis of non-stationary modulation processes. It enables to detect and to follow the variations of an "instantaneous" frequency of an oscillatory component of radiation.

An important role in the present work belongs also to the method, used for the detection of quasi-periodic features in the time records of the solar microwave radiation intensity. It consists in application of an original data analysis algorithm (Shkelev et al., 2002; Zaitsev et al., 2001b) made as a combination of the "sliding window" Fourier (SWF) transform technique

and the nonlinear Wigner-Ville (WV) method (Cohen, 1989; Ville, 1948; Wigner, 1932). Below we outline the idea of this data analysis algorithm and its main features.

The classical Fourier transform enables the analysis of a given signal in terms of separate spectral frequency components. It is applied for the study of relative distribution of energy between the spectral components in the case of sufficiently long (ideally infinite) duration of the analyzed signal. However such energetic spectrum does not provide an information on a time when each particular spectral component appears. Possible improvement of the classical Fourier transform method in that respect consists in its application within a certain interval of time Δt (so called "window") and in a consequent shift of this "window" along the time axis. This approach became a standard method for the analysis of non-stationary signals. Further generalization of SWF transform method leads to the wavelet analysis, where effect of the "window" is produced by means of a certain mother-wavelet function. Wavelet transform enables judging about energy distribution over the time and frequency of an analyzed signal. Nowadays this method is also widely used for the analysis of non-stationary and impulsive signals. Its efficiency is however strongly dependent on parameters of the applied mother-wavelet function, which needs to be specially selected and adjusted to the type of particular analyzed signal.

Recently one more spectral analysis method has been applied in astrophysics. This method is based on the Wigner-Ville (WV) transform

$$P(f, t) = \int_{-\infty}^{\infty} z\left(t + \frac{\tau}{2}\right) z^*\left(t - \frac{\tau}{2}\right) e^{-i2\pi f\tau} d\tau, \quad (5)$$

where $z(t) = s(t) + is_H(t)$ is an analytic signal, made of the analyzed sample of real signal $s(t)$, and its Hilbert conjugate $s_H(t)$. Function $P(f, t)$ gives distribution of the signal energy over frequency f and time, and may be visualized in the form of a dynamical spectrum of the signal. According to its definition (5), WV transform may be also interpreted as Fourier image (relative the shifted time) of the local autocorrelation function for the analytical signal $z(t)$.

Since the time t appears explicitly among the arguments of the WV spectrum $P(f, t)$, this method is most efficient for high-resolution spectra-temporal analysis of non-stationary signals with varying spectra, such as quasi-harmonic signals with a changing frequency, or varying impulsive signals. In these cases SWF transform and wavelet methods are less efficient, because the averaging over the analysis window (or over the wavelet) results in a decrease of spectral density of the signal components, varying within the corresponding time intervals. At the same time, the non-linearity and non-locality of WV method cause appearance of artificial inter-modulation spectral components at combination frequencies (artifacts) and may result also in suppression of weak spectral components of the signal by its more intense or noisy parts (Cohen, 1989; Shkelev et al., 2002). To compensate the drawbacks of SWF and WV data analysis methods, when they are used separately, and to keep their strong features, the methods were combined in a proper way in the SWF-WV algorithm, which uses various types of signal processing and filtration (with variable shape and size of the analysis windows) in order to eliminate possible artifacts and to provide high spectral and temporal resolution (Kislyakov et al., 2011; Shkelev et al., 2002).

To avoid the appearance of spurious spectra caused by the signal edge effects in the case of analysis of real finite in time signal samples, the so called "weighting" functions with smoothed edges are used. In the present study, the SWF spectrum S_k of a discrete signal

s_n consisting of N counts is calculated by a discrete Fourier transform (DFT) (Allen & Mills, 2004; Marple, 1986):

$$S_k = \sum_{n=0}^{N-1} \text{wnd}(n) s_n \exp \left\{ -i \frac{2\pi nk}{N} \right\}, \quad k = 0, 1, \dots, N-1 \quad (6)$$

with a sliding window $\text{wnd}(n)$. The following window functions are used (see also Pollock (1999)):

$$\begin{aligned} \text{wnd}_1(n) &= \begin{cases} 1, & 0 \leq n < N \\ 0, & n \geq N \end{cases} && \text{– a rectangular window} \\ \text{wnd}_2(n) &= \begin{cases} \cos^2 \left(\frac{\pi \cdot n}{2N} \right), & 0 \leq n < N/2 \\ 0, & n \geq N/2 \end{cases} && \text{– Henning's window} \\ \text{wnd}_3(n) &= \begin{cases} 1 - 6 \cdot \left(\frac{2 \cdot n}{N} \right)^2 + 6 \cdot \left(\frac{2 \cdot n}{N} \right)^3, & 0 \leq n < N/4 \\ 2 \cdot \left(1 - \frac{2 \cdot n}{N} \right)^3, & N/4 \leq n < N/2 \\ 0, & n \geq N/2 \end{cases} && \text{– Parsen's window.} \end{aligned} \quad (7)$$

The advantage of this method consists in its high performance speed, especially if the standard algorithms of fast Fourier transform (FFT) are used in the calculations (Allen & Mills, 2004; Marple, 1986). On the other hand, frequency resolution of SWF is reverse proportional to the number of signal counts in the applied window. Therefore the size of window should be sufficiently large. This in its turn decreases the temporal resolution of the method. In practice, the choice of particular type and width of the window is determined by dynamical features of the analyzed signal.

An algorithm of the discrete WV transform is determined by the following expression:

$$P_{mk} = P(m\Delta t, k\Delta f) = 2\Delta t \sum_{n=0}^{2N-1} \left[z_{m+n} z_{m-n}^* \exp \left\{ -i \frac{\pi nk}{N} \right\} \right], \quad \{m, k\} = 0, 1, 2, \dots, 2N, \quad (8)$$

where z_n and z_n^* are discrete values of the analyzed complex analytical signal made, as determined above, of the real discrete signal and its Hilbert conjugate; Δt is a period of discretization, and $\Delta f = 1/(4N\Delta t)$ is the frequency step. Note, that WV transform results in real values only in the case of continuous functions integrated in infinite limits (like in (5)). The discrete WV transform (8) yields a complex function P_{mk} , which is called as "pseudo-WV transform" (Cohen, 1989). In that respect in practice only a module of P_{mk} or its real part are considered.

In course of the comparative study performed in Kislyakov et al. (2011); Shkelev et al. (2002) it has been shown that WV data analysis technique enables higher spectral and temporal resolution than that of the SWE. In Shkelev et al. (2002) the efficiency of WV and SWF methods was checked with various test signals, made as combinations of impulsive and quasi-harmonic processes. By this, along with the meaningful spectrum, WV transform generated specific artificial spectral features (due to the non-linearity of the method). It has been shown in that respect that superimposing of the higher resolution WV spectra with those of lower resolution provided by SWE, may help to identify and to exclude these artificial spectral features from the consideration. Altogether, combined with each other the described

above SWF and WV methods provide an efficient data analysis algorithm characterized by high sensitivity, high spectral and temporal resolution, and ability to detect complex multi-signal modulations in the analyzed data records, enabling the dynamical spectra of these modulations. For successful operation of the SWF-WV algorithm, the sampling cadence of analyzed data series should provide sufficient number of the data points, e.g. $\geq 10,000$ points per realization. The length of the analyzed data series should be consistent with the time scales of considered dynamic phenomena, i.e. the duration of an analyzed data set should include at least several periods of the modulating oscillatory component. The SWF-WV method appears the most efficient for the study of signals with non-stationary complex modulations. In such cases the traditional Fourier transform and wavelet methods are less efficient. This feature of the algorithm has been, in particular, used to distinguish between the modulations, possibly caused by the large-scale transverse quasi-periodic motion of the loops, which are the subject of the present study, and the modulations with frequency drifts related with the electric current LCR-oscillations in the loops.

For the visualization of the whole variety of the detected modulations, so called averaged spectral density plots are produced along with the dynamic spectra by the SWF-WV algorithm. These plots are obtained by averaging of multiple instantaneous cuts of the dynamic spectrum taken at given moments of time, so that short-living modulation features also become clearly seen among the longer lasting modulation lines. These both types of spectra (dynamic and averaged) enable the detection of the large-scale transverse oscillatory dynamics of the radiating coronal magnetic loops.

The universality of SWF-WV algorithm resulted in its successful application in different branches of space physics. The algorithm was used for the diagnostics of intrinsic physical and dynamical conditions in the stellar and planetary systems, solar/stellar winds, as well as in solar and planetary radiation sources and planetary environments (Khodachenko et al., 2006; Kislyakov et al., 2006; Panchenko et al., 2009; Zaitsev et al., 2003; 2004). Nowadays, the link to SWF-WV data analysis algorithm is available for the scientific community via the on-line catalogue of models and data analysis tools (<http://europlanet-jra3.oeaw.ac.at/catalogue/>), developed within the JRA3-EMDAF (European modelling and data analysis facilities) activity (<http://europlanet-jra3.oeaw.ac.at/>) of the European FP7 research infrastructure project Europlanet-RI.

4. Diagnostics of large-scale oscillations of coronal loops by the analysis of VLF modulations of microwave radiation

5. Instrumentation and modulations detection capabilities

We analyze the VLF (< 0.01 Hz) modulations of solar microwave bursts recorded in Metsähovi Radio Observatory (Finland) with the 14-m and 1.8 m radio telescope antenna at 37 GHz and 11.7 GHz, respectively. The key selection criterion for the analyzed microwave data was their synchronism with the oscillating loops observed in extreme ultraviolet (EUV) by TRACE (Aschwanden et al., 2002). The width of the antenna beam pattern of the Metsähovi radio telescope at 37 GHz is $2.4'$, the sensitivity of the receiver is about 0.1 sfu (10^{-23} W m⁻² Hz⁻¹), and time resolution, $0.05 \div 0.1$ s. Therefore, at 37 GHz the spatial resolution of the radio telescope is sufficient for identification of an active region that contains a radiating source. This enables to analyze microwave radiation emitted directly from the region, imaged in EUV (e.g., observed by TRACE), and to perform the comparison of the radiation features

and dynamics of coronal loops. At 11.7 GHz the radiation is collected from the whole solar disk and the position of the radiating source cannot be resolved. However, even in this case, by comparison with observations in other wavelengths and timing of the events, it is usually possible to identify the microwave radiation features related to the energy release and dynamic phenomena in particular active regions.

Variations of the background magnetic field in a radiating source may cause not only the amplitude modulation of microwave radio emission from solar active regions (according (1)), but also could result in a certain frequency modulation (due to the dependence of electron gyro-frequency ν_B on the magnetic field). The estimated width of the gyro-frequency variation interval due to this effect is from several tens to several hundreds MHz. At the same time, the bandwidth of the receiver at Metsähovi is much larger than this interval and a possible frequency modulation of the microwave radio emission cannot be resolved. Thus, one can detect only the effects of varying magnetic field, manifested in the intensity modulation of the microwave signal, due to (1).

5.1 Observations and interpretation

In this subsection, we show how the analysis of long-periodic modulations of solar microwave radiation accompanying the explosive events on the Sun may be used to obtain information on the details of large-scale dynamics of the coronal loops associated with flares and the overall structure of solar active regions. By this, the primary focus here is made on VLF modulations of the radiation, emitted from active regions where TRACE observed in EUV at the same time the large-scale oscillations of coronal loops. Careful check of the solar microwave radio emission records available at Metsähovi revealed several events which coincide in time with the EUV observations of oscillating coronal loops. Below these events are considered in details.

Figure 3c shows the intensity profile and dynamic spectrum of VLF modulations of microwave emission from the active region AR8910 on the limb (see Figure 3a,b) where a group of oscillating loops (Figure 4a) was observed by TRACE after M2.0 flare on 2000-Mar-23, at 11:30-12:00 UT (Aschwanden et al., 2002). These observations were performed at 37 GHz, and the spatial resolution of the Metsähovi radio telescope was sufficient to resolve the radiating source in the active region AR8910.

A remarkable feature of the VLF modulation dynamic spectrum in Fig. 3c,d and the averaged spectral density plot in Fig. 3d consists in the presence of several "modulation pairs". These are the modulations (a) at 1.7 mHz (~ 10 min) and 3.4 mHz (~ 4.9 min); (b) at 6.0 mHz (~ 2.8 min) and 12.0 mHz (~ 1.4 min), as well as (c) at 7.8 mHz (~ 2.1 min) and 15.6 mHz (~ 64 s). According to the considerations in Section 2, these "modulation pairs" could indicate the transverse oscillating loops with the periods, corresponding to the main frequencies of the pairs, i.e. ~ 10 min; ~ 2.8 min, and ~ 2.1 min for the cases (a), (b), and (c), respectively. By this, the first "modulation pair" (case (a)) as a signature of the loop transverse oscillation with a period ~ 10 , fits quite well the results of TRACE observations, which found the oscillating loop with approximately the same period (615 s) (Aschwanden et al., 2002; Schrijver et al., 2002). As it can be seen from the dynamical spectrum in Figure 3c, the spectral resolution of the analysis performed in this particular case was about 0.3 mHz. By this, the frequency 1.62 mHz corresponding to the detected TRACE period of 615 s is definitely within the frequency

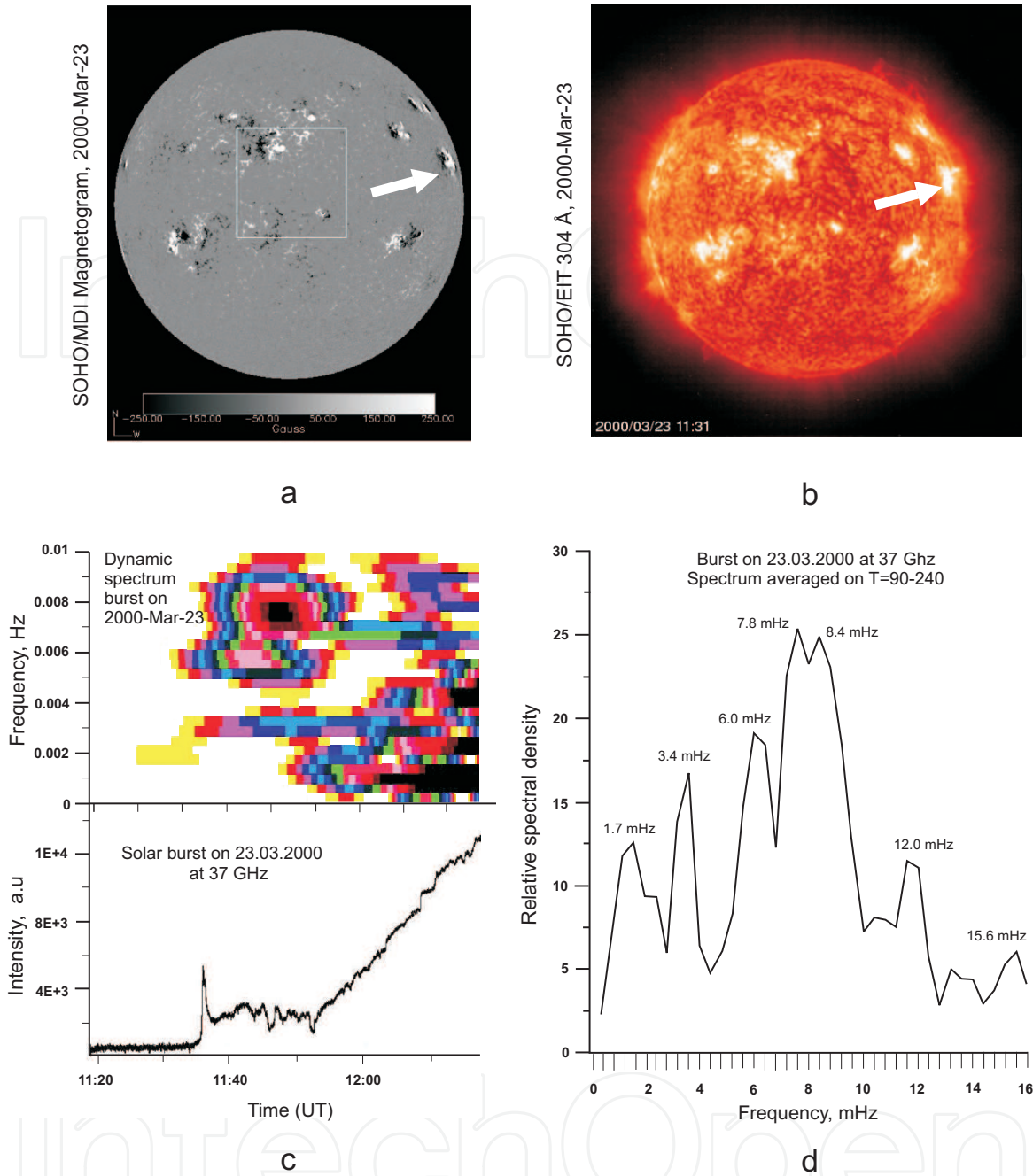


Fig. 3. (a) SOHO/MDI Magnetogram of the Sun on 2000-Mar-23, white arrow points at the active region AR8910; (b) The Sun image in 304 Å on 2000-Mar-23 from SOHO/EIT, white arrow points at the active region AR8910; (c) Intensity profile and corresponding VLF modulation dynamic spectrum of the microwave radiation, recorded from the active region AR8910 on 2000-Mar-23, at 11:30-12:00; Color codes the dynamic spectral relative intensity (arbitrary units), more dark features correspond to stronger (better pronounced) modulations; (d) averaged spectral density of the VLF modulation.

interval 1.7 ± 0.3 mHz of the modulation feature revealed by the analysis of the microwave radiation.

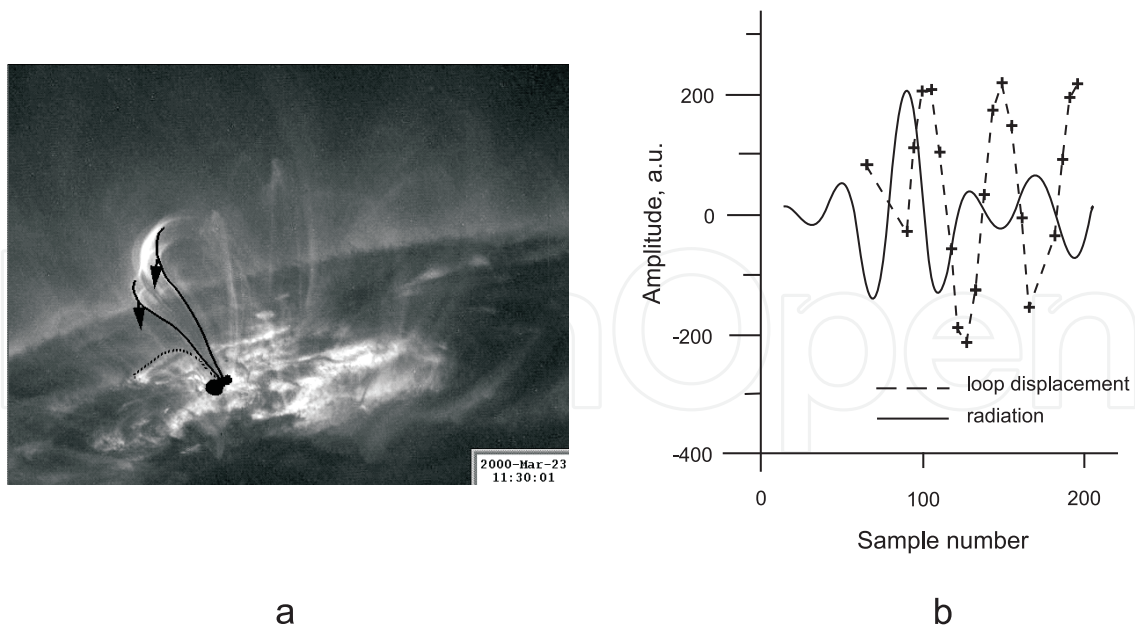


Fig. 4. (a) Transverse oscillating coronal loops observed by TRACE in the active region AR8910 after an M2.0 flare on 2000-Mar-23 at 11:30-12:00 UT (Aschwanden et al., 2002); (b) Phase comparison of the ~ 10 min modulation component of the microwave emission on 2000-Mar-23 and the amplitude of the corresponding 615 s oscillation of the TRACE loop.

A higher level of the second harmonic in the modulation pair 1.7 mHz (~ 10 min) and 3.4 mHz (~ 4.9 min) is very likely due to the fact that in this particular case two different mechanisms, modulating the microwave emission of the loop, are by chance manifested simultaneously. The first mechanism is that considered in this paper, which is connected with a large-scale transverse oscillation of the loop. The second mechanism is due to the parametric resonance between 5-min velocity oscillations in the solar photosphere and acoustic oscillations of coronal magnetic loop modulating the microwave emission (Zaitsev et al., 2008). The effect consists in simultaneous excitation in the loop, which occasionally appeared to have a resonant frequency close to 10 min, of oscillations with periods ~ 5 min, ~ 10 min, and ~ 3 min, which correspond to the 5-min pumping frequency of the photospheric convection velocity oscillations, subharmonic, and the first upper frequency of the parametric resonance, respectively (Zaitsev et al., 2008; Zaitsev & Kislyakov, 2006).

It makes no sense to search in TRACE data for the signatures of other oscillating loops (cases (b) and (c)), indicated by the VLF modulations of the microwave radiation during the 2000-Mar-23 event, since with the usual 40 s image sampling cadence of TRACE and the 4-point resolution limit of the instrument (Aschwanden et al., 2002) the fastest detectable by TRACE period is about 3 min. The remaining short-periodic "non-paired" modulation feature at 8.4 mHz (~ 1.9 min) may also be a part of a "modulation pair", of which the second harmonic counterpart could not be resolved in the VLF spectrum due to the strong contamination of the analyzed microwave signal. Such weak higher harmonic components may be as well a signature of another oscillatory process, which is unrelated to the large-scale transverse motion of loops, e.g., a sausage-type MHD wave excited in a loop. Detailed analysis of this special case remains however beyond the scope of the present study.

An additional confirmation of the fact that ~ 10 min modulation of the microwave radiation emitted from the active region AR8910 on 2000-Mar-23, is connected with the transverse

oscillatory motion of a coronal loop, shown in Fig. 4a, and that it is in very likely related to the motion of the emission diagram pattern, comes from the graphs in Fig. 4b. This figure enables phase comparison for the transverse motion of the loop (observed with TRACE Aschwanden et al. (2002)) and the filtered 1.7 mHz (~ 10 min) component of the radiation. The last characterizes temporal behaviour of the radio emission received from the oscillating loop. The shifted phase ($\sim \pi$) means that the maxima and minima of the radiation part controlled by the loop motion correspond to the specific orientations of the loop and are connected with a certain direction of the emission diagram relative to the observer.

The microwave burst on 2001-Sep-07 represents another example of manifestation of the coronal loop transverse oscillations in modulation of solar radio emissions. The burst was produced during M-flare activity at 15:30 UT in the active region AR9601, close to the solar disc center (see Figure 5a,b), where TRACE observed a group of oscillating loops, immediately after the flare (Aschwanden et al., 2002). The corresponding microwave radiation record was made at 11.7 GHz with the Metsähovi radio telescope. At this frequency, the Metsähovi antenna cannot resolve the position of a radiating source, and the emission from the whole solar disk contributed to the analyzed microwave intensity profile. At the same time, as can be seen in Fig. 5c, which presents the analyzed microwave radiation record with the burst and its VLF modulation dynamic spectrum, the spectral features related to the processes in the flaring active region AR9601 can easily be identified by timing of the event. In particular, the dynamic spectrum of VLF modulations of the microwave radiation exhibits several lines, which start simultaneously with the impulsive phase of the flare (at 15:30 UT). These may be the signatures of different oscillating loops excited by the flare. By this, most of the oscillations (e.g. the dynamic spectrum lines) decay at the time intervals > 20 min. Unfortunately for this particular event it is impossible to determine exact duration of each of these decaying modulations because the available microwave radiation record does not cover the end of the event. As it can be seen in Fig. 5c, some of the dynamic spectrum lines continue beyond the analyzed record time frame.

Three "modulation pairs" can be identified in the dynamic and averaged spectra in Fig. 5c,d: (a) 1.8 mHz (~ 9.2 min) and 3.6 mHz (~ 4.6 min); (b) 2.7 mHz (~ 6.2 min) and 5.4 mHz (~ 3.1 min); as well as (c) 4.3 mHz (~ 3.8 min) and 8.6 mHz (~ 1.9 min), which may be the signatures of transverse oscillating loops with periods ~ 9.2 min, ~ 6.2 min, and ~ 3.8 min, respectively. We note that the loop periods in the cases (a) and (b) are consistent with the 6-10 min oscillating loops observed with TRACE (Aschwanden et al., 2002), whereas the shorter period oscillation (case (c)) cannot be resolved by TRACE because of the relatively long image sampling cadence. The modulation at 5.4 mHz (~ 3.1 min) may also be a weak third harmonic produced by the 9.2 min oscillating loop. If this is true, then the line at 2.7 mHz (~ 6.2 min) will have no a pair-companion, and one should exclude the possibility of the ~ 6.2 min transverse oscillating loop. A "non-paired" weak modulation feature at 6.4 mHz (~ 2.6 min) may be a signature of an oscillating loop with not resolved second harmonic. At the same time, as for the 2000-Mar-23 event, weak short-period harmonics may be the signatures of oscillatory processes that are unrelated to the transverse motion of a loop, but caused only by a changing magnetic field in the radiating source.

The strong modulation line at 0.6 mHz (~ 27.7 min) should be considered separately from all other modulations mentioned above. The dynamical spectrum in Fig. 5c, as well as a separate study of VLF modulations of the microwave radiation recorded before the flaring burst at 15:30 UT, reveal the presence of the ~ 27.7 min component also before the flare. In view of the fact

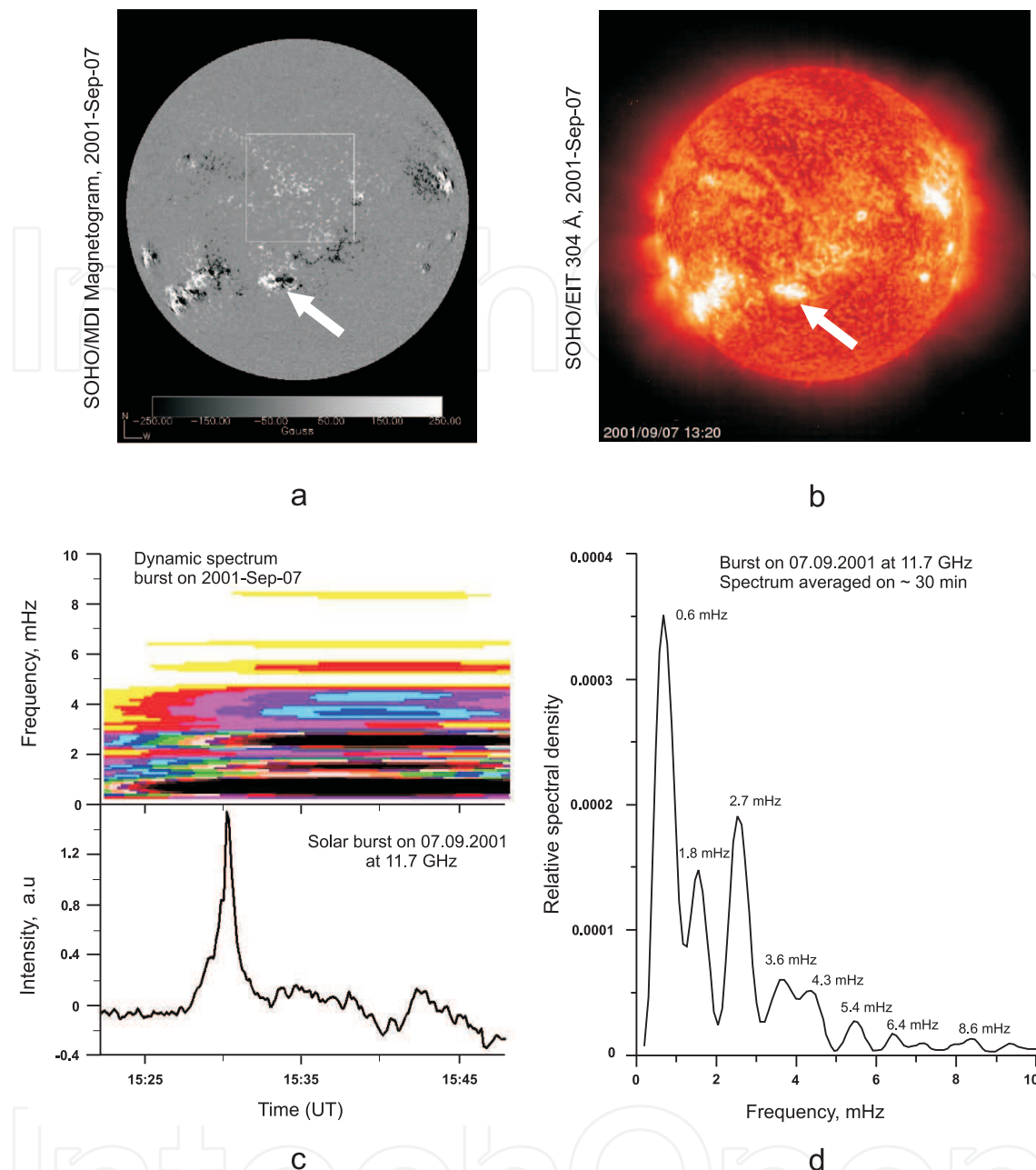


Fig. 5. (a) SOHO/MDI Magnetogram of the Sun on 2001-Sep-07, white arrow points at the active region AR9601; (b) The Sun image in 304 Å on 2001-Sep-07 from SOHO/EIT, white arrow points at the active region AR9601; (c) Intensity profile and corresponding VLF modulation dynamic spectrum of the microwave burst on 2001-Sep-07, at 15:30-15:50 associated with an M-flare in the active region AR9601; Color codes the dynamic spectral relative intensity (arbitrary units), more dark features correspond to stronger (better pronounced) modulations; (d) averaged spectral density of the VLF modulation.

that the analyzed microwave emission (at 11.7 GHz) was received from the whole solar disk, the ~ 27.7 min modulated part of radiation very likely originates in another active region. It may also be connected with a kind of global solar seismology process.

The last example of possible manifestation of transverse oscillations of coronal loops in microwaves which we present here, is the event on 2001-Sep-15, when TRACE observed oscillating loops, associated with M flare at 11:23 UT in the active region AR9608, close to the limb (see Figure 6a,b). Similar to the case of the microwave burst on 2001-Sep-07, the event on 2001-Sep-15 was observed at 11.7 GHz, and the microwave radiation source in AR9608 was not resolved by the Metsähovi antenna. Thus, the emission from the whole solar disk contributed to the analyzed microwave intensity profile. However, as for the burst on 2001-Sep-07, all the spectral features related to the flaring active region AR9608 can be identified by event timing. As it can be seen in Fig. 6c, the dynamic spectrum of VLF modulations of the microwave radiation consists of several lines, most of which begin simultaneously with the impulsive phase of the flare at 11:23 UT. These lines may be associated with oscillatory processes in the active region loops triggered by the flare. All the post-flare oscillations decay at the time intervals from ~ 20 min up to ~ 1 hour.

Fig. 6d shows the averaged spectral density of the VLF modulations of the microwave burst on 2001-Sep-15. At least one "modulation pair": 1.3 mHz (~ 12.8 min) and 2.6 mHz (~ 6.4 min) can be identified among the detected modulation lines. It is very likely connected with a transverse oscillating loop having the period ~ 12.8 min. This result agrees with the reported TRACE observations of the oscillating loop in the active region AR9608 with a period $\sim 12 - 15$ min. Other detected in the microwave record on 2001-Sep-15 (see Fig. 6c,d), more short-periodic modulations at 3.8 mHz (~ 4.4 min) and 5.2 mHz (~ 3.2 min) could be higher-order harmonics produced by the 12.8 min oscillating loop, or the modulations associated with oscillatory processes not connected with the transverse motion of loops. They may also be the signatures of oscillatory processes in small loops, which cannot be seen in the TRACE EUV movies due to the limitations of the operated observing mode. Additionally should be mentioned a relatively weak line at 0.7 mHz (~ 23.8 min). Its possible second harmonic could contribute to the broad line near 1.3 mHz, which is identified as a main frequency line in another modulation pair. If that is the case, then this may be a signature of another transverse oscillating loop with the period ~ 23.8 min. Verwichte et al. (2010) reported recently detection of such an oscillating loop related with the considered flaring event in the active region AR9608.

A special remark deserves also the long lasting ultra-low-frequency (ULF) modulation at 0.3 mHz (~ 56 min), clearly visible in both, the dynamic and averaged, spectra of the long-periodic modulations of solar microwave radiation on 2001-Sep-15 in Figs. 6c,d. Similarly to the 27 min line in the case of the 2001-Sep-07 burst, this ULF modulation appears before the flaring burst and lasts much longer than all other modulation lines in the spectrum (Fig. 6c). Therefore, it cannot be related to the flare in the active region AR9608 and consequent post-flare dynamics of coronal loops. This modulation feature is probably connected with the solar seismology processes, or a slow dynamics of another active region. As an additional argument in support of the solar global i.e., helioseismic nature of the ULF ($\nu_0 < 0.6$ mHz, i.e. $\tau > 30$ min) modulations may be the fact that these modulations are usually detected in the radiation records made at 11.7 GHz when the radio emission from the whole solar disk contributes to the analyzed microwave intensity profile. The radiation emitted from the spatially resolved separate active regions, for example, at 37 GHz with Metsähovi radio telescope, does not exhibit any ULF modulation features. In more details the ULF modulations of solar microwave radiation are considered in Kislyakova et al. (2011).

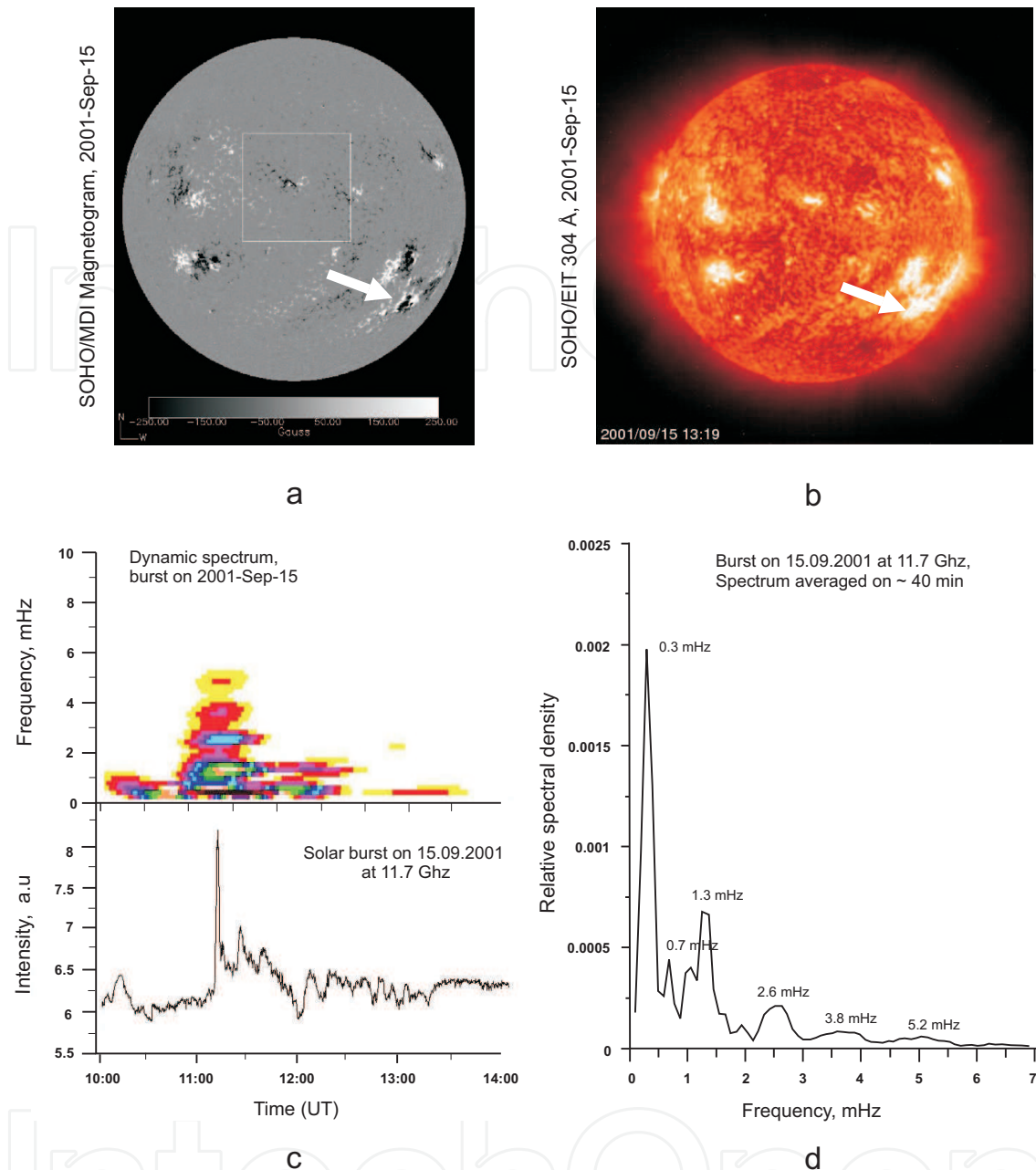


Fig. 6. (a) SOHO/MDI Magnetogram of the Sun on 2001-Sep-15, white arrow points at the active region AR9608; (b) The Sun image in 304 Å on 2001-Sep-15 from SOHO/EIT, white arrow points at the active region AR9608; (c) Intensity profile and corresponding VLF modulation dynamic spectrum of the microwave burst on 2001-Sep-15, at 11:23-12:15 associated with an M-flare in the active region AR9608; Color codes the dynamic spectral relative intensity (arbitrary units), more dark features correspond to stronger (better pronounced) modulations; (d) averaged spectral density of the VLF modulation.

5.2 On the magnetic field variations, estimated from VLF spectra

It is impossible, using the available data, to perform an exact calculation for the amplitude of magnetic field variations. That is because the analyzed microwave signals were recorded in relative units without calibration to the radiation intensity scale. At the same time, taking into account known values of the maximal intensity measured during the radio

bursts and the lower limit of sensitivity of the Metsähovi receiver, the intensity modulation amplitude ΔI_ν can be estimated roughly from the obtained VLF spectra, by their comparison with the spectra of specially created modelling signals (Khodachenko et al., 2005). For the considered in the paper events this estimation gives the value of the relative variation of intensity $\Delta I_\nu / I_\nu^0 \sim 10^{-2} \div 10^{-1}$. Assuming, as an upper rough limit, that this variation of intensity is connected only with the varying magnetic field, we come to a relation $\Delta I_\nu / I_\nu^0 = (B/B_0)^\gamma - 1 = ((\Delta B/B_0 + 1)^\gamma - 1)$, where $\Delta B/B_0$ is the relative variation of magnetic field, and $\gamma = -0.22 + 0.9\delta$ is the power index of magnetic field in the equation (1). For $2 < \delta < 7$ one gets that $\gamma = 1.58 \div 6.08$. For the case of small relative variations of the magnetic field we finally obtain $\Delta I_\nu / I_\nu^0 \approx \gamma \Delta B/B_0 = 10^{-2} \div 10^{-1}$, which for $B_0 = 100\text{G}$ gives the amplitude $\Delta B = (0.16 \div 6.3) \text{G}$.

6. Discussion, conclusions and perspectives

The analysis of VLF modulations of solar microwave bursts presented in this work shows good temporal coincidence of the modulations and their oscillatory parameters with the observed decaying large-scale transverse oscillations of the coronal loops triggered by flares. This indicates about a physical link between the oscillatory motion of the loops and variations of the observed radio emission. As a working hypothesis to take this link into account, a loop with the propagating beams of non-thermal particles which produce microwave emission due to the electron gyro-synchrotron mechanism, has been considered. As pointed out by Schrijver et al. (2002), who considered several cases of transverse oscillations of coronal loops observed with TRACE (including the event on 2000-Mar-23 addressed in the present paper), in almost all cases the oscillating loops lie at, or near, the large-scale separatrices, or near the sites involved in reconnection. These regions may be the sources of non-thermal particles injected into the loops and generating microwave emission there. Moreover, in the case on 2000-Mar-23 the loop oscillation happened in response to a flaring event located at the loop base Schrijver et al. (2002). That could provide a direct input of energetic particles into the loop.

In the most general case, thermal bremsstrahlung mechanism of the radiation should be also considered, besides of the gyro-synchrotron, for the analyzed frequency range of the solar microwave emission. If the last mechanism assumes that there are high energy electrons passing through the magnetic loop, the first one is connected with the radiation of hot plasma heated by the electron beams in the chromospheric footpoints of the loop. A comparative study of contribution of the bremsstrahlung and gyro-synchrotron radiation to the microwave emission of a flare, performed in Urpo et al. (1994), shows that thermal bremsstrahlung is more important for the microwave events that have an intensity of the order of or less than 100 SFU, with the exception of cases when the electron spectrum is sufficiently hard. Therefore, correct interpretation of the microwave radiation source requires consideration of both mechanisms, for example by involving of the hybrid thermal/nonthermal model of the solar flare emission (Holman & Benka, 1992). However, looking at a possibility of an oscillatory behaviour of the microwave radiation source which constitutes the primary subject of the present study, we notice that in the case of the bremsstrahlung mechanism it is possible only for a varying energy deposition into the system, i.e. a varying flow of non-thermal particles heating the loop footpoints. In view of the unclearness of how the post-flare transverse oscillating loop may modulate the source of accelerated electrons, we built our analysis with the assumption that the non-thermal particle population remains

more-or-less stable, and all the variations of the observed microwave radiation are connected with the non-thermal gyro-synchrotron part of the radiation, modulated by the large-scale oscillatory motion of the loop. The bremsstrahlung component, even being present in the microwave radiation, does not contribute to the analyzed oscillating part of the emission provided by the gyro-synchrotron mechanism.

Our analysis here is based on the assumption of an optically thin microwave source. In this case the radiation intensity is proportional to emissivity η_ν , given by equation (Dulk, 1985)

$$\eta_\nu \approx 3.3 \times 10^{-24} 10^{-0.52\delta} N B (\sin \theta)^{-0.43+0.65\delta} \left(\frac{\nu}{\nu_B} \right)^{1.22-0.9\delta}, \quad (9)$$

where ν is radiation frequency, N is the number of electrons per cubic centimeter with energy higher than 10 keV, B is magnetic field, $\nu_B = eB/(2\pi m_e c)$, is the electron-cyclotron frequency, and δ is the electron energy spectrum index. This fact has been used for obtaining our basic equation (1) in Section 1. In the opposite case of an optically thick source, the intensity of microwave radiation is proportional to the effective temperature T_{eff} , i.e., to the ratio of emissivity η_ν and absorption coefficient κ_ν . For the last, Dulk (1985) provides the following expression:

$$\kappa_\nu \approx 1.4 \times 10^{-9} 10^{-0.22\delta} (N/B) (\sin \theta)^{-0.09+0.72\delta} \left(\frac{\nu}{\nu_B} \right)^{-1.3-0.98\delta}. \quad (10)$$

Therefore, in the case of an optically thick source the dependence of radiation intensity on the varying magnetic field $B(t)$ and direction to the observer $\Theta(t)$ will be different than that given by the equation (1). However, the character of this dependence, i.e. $I_\nu \propto (\sin(\Theta(t)))^k B(t)^l$, where k and l are the numbers depending on the non-thermal electron spectral index δ , will remain the same. Therefore, one may expect similar manifestation of the varying $B(t)$ and $\Theta(t)$ in the modulation of the received microwave emission also in the case of an optically thick source.

Analysis of LF and VLF modulations of solar microwave radiation is a relatively new direction in solar radio astronomy which appears nowadays a subject of a certain interest. VLF variations of solar microwave radiation intensity may be related to slow variations of magnetic field in a radiating source, as well as to large-scale motions of coronal structures containing the radiating source. Joint action of two radiation modulating factors: (i) the quasi-periodic fluctuation of magnetic field and (ii) motion of the radio emission diagram, in the case of a transverse oscillating coronal loop results in essentially non-sinusoidal (non-harmonic) character of the signal received by a remote observer, with strongly pronounced two first harmonics (at the main and double frequency of the oscillation), called here as "modulation pairs". Such specifics of the VLF spectrum has been used for the identification of transverse oscillating loops triggered by flares. The analysis of solar microwave records has been performed with an algorithm based on Sliding Window Fourier transform and Wigner-Ville techniques. This high sensitive algorithm provides, significant spectral and temporal resolution which enable clear detection of VLF "modulation pairs" in the solar flaring microwave radiation (microwave bursts). Comparison of parameters of these "modulation pairs" with the simultaneous TRACE observations in EUV of the corresponding solar active regions enabled to associate some of the paired VLF modulation features with the large-scale transverse oscillations of coronal loops. The "non-paired" features also detected

in the VLF modulation dynamic spectra, may be either parts of "modulation pairs" in which the second harmonic cannot be resolved because of the strong contamination of the analyzed signal, or be the signatures of other oscillatory processes (MHD modes) in the loops, unrelated to their large-scale transverse motion, e.g., sausage-type MHD waves.

The presence of "modulation pairs" in the VLF spectra of solar microwave radiation is considered here as an indication of the transverse oscillating coronal loops. However, the exact characterization of the transverse motion of radiating loops by the dynamical spectra of microwave emission needs a quantitative analysis of the measured radio signal and superimposing these results with a precise calculation of the radiation from the loop, taking into account the loop position relative observer. This topic requires a dedicated study. It outlines the general direction for further development of the ideas expressed in the paper.

Besides of that, of certain interest appear the long lasting ULF modulations of solar microwave radiation detected at < 0.6 mHz (> 30 min) in the absence of bursts, i.e. during the periods of quiet Sun. It is remarkable that these modulations are not visible in the emissions from separate active regions, recorded in particular at 37 GHz with Metsähovi radio telescope. But they appear in the integrated radiation received from the whole solar disk at 11.7 GHz. This fact may be considered as an argument in support of the global helioseismic nature of these ULF modulations, which also require further more detailed study.

7. Acknowledgements

This work was supported by the Austrian Fond zur Förderung der wissenschaftlichen Forschung (project P21197-N16). The authors are thankful to the JRA3/EMDAF (European Modelling and Data Analysis Facility; <http://europlanet-jra3.oeaw.ac.at>) – a subdivision of the European research infrastructure EUROPLANET-RI and EU FP7 project IMPEx (<http://impex-fp7.oeaw.ac.at>) for the support of their research communication and collaboration visits. The authors would like to thank M.Aschwanden for useful discussions and the data regarding the transverse large-scale dynamics of coronal loops.

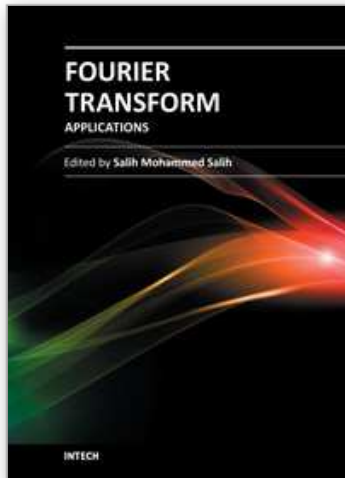
8. References

- Allen, R.L. & Mills, D.W. (2004). *Signal analysis: time, frequency, scale, and structure*. IEEE Press, Wiley-Interscience, ISBN:0-471-23441-9.
- Aschwanden, M.J.; Fletcher, L.; Schrijver, C.J.; Alexander, D. (1999). Coronal Loop Oscillations Observed with the Transition Region and Coronal Explorer. *The Astrophysical Journal*, Vol. 520, No. 2, 880–894, (DOI:10.1086/307502).
- Aschwanden, M.J. (2002). Particle acceleration and kinematics in solar flares - A Synthesis of Recent Observations and Theoretical Concepts (Invited Review). *Space Science Review*, Vol. 101, No. 1, 1–227, (DOI:10.1023/A:1019712124366).
- Aschwanden, M.J.; DePontieu, B.; Schrijver, C.J.; Title, A. (2002). Transverse Oscillations in Coronal Loops Observed with TRACE II. Measurements of Geometric and Physical Parameters. *Solar Physics*, Vol. 206, No. 1, 99–132, (DOI:10.1023/A:1014916701283).
- Cargill, P.J.; Goodrich, C.C.; Vlahos, L. (1988). Collisionless shock formation and the prompt acceleration of solar flare ions. *Astronomy and Astrophysics*, Vol. 189, No. 1-2, Jan., 254–262, ISSN 0004-6361.
- Cohen, L. (1989). Time-frequency distributions - A review. *IEEE Proc.*, Vol. 77, July-1989, 941–981, ISSN 0018-9219.

- Dulk, G.A. (1985). Radio emission from the sun and stars. IN: *Annual review of astronomy and astrophysics*, Vol. 23(A86-14507 04-90), 169–224, Palo Alto, CA, Annual Reviews, Inc., (DOI:10.1146/annurev.aa.23.090185.001125).
- Dulk, G.A. & Marsh, K.A. (1982). Simplified expressions for the gyrosynchrotron radiation from mildly relativistic, nonthermal and thermal electrons. *The Astrophysical Journal*, Vol. 259, Aug-1982, 350–358, (DOI:10.1086/160171).
- Hardy, S.J.; Melrose, D.B.; Hudson, H.S. (1998). Observational tests of a double loop model for solar flares. *Publications Astronomical Society of Australia*, Vol. 15, No. 3, 318–324.
- Holman, G.D. & Benka, S.G. (1992). A hybrid thermal/nonthermal model for the energetic emissions from solar flares. *The Astrophysical Journal*, Vol. 400, No. 2, L79–L82, ISSN 0004-637X, (DOI:10.1086/186654).
- Holman, G.D. & Pesses, M.E. (1983). Solar type II radio emission and the shock drift acceleration of electrons. *The Astrophysical Journal*, Vol. 267, No. 15, 837–843, ISSN 0004-637X, (DOI:10.1086/160918).
- Karlický, M. & Kosugi, T. (2004). Acceleration and heating processes in a collapsing magnetic trap. *Astronomy and Astrophysics*, V. 419, 1159–1168, (DOI:10.1051/0004-6361:20034323).
- Khodachenko, M.L.; Haerendel, G.; Rucker, H.O. (2003). Inductive electromagnetic effects in solar current-carrying magnetic loops. *Astronomy and Astrophysics*, Vol. 401, 721–732, (DOI:10.1051/0004-6361:20030146).
- Khodachenko, M.L.; Zaitsev, V.V.; Kislyakov, A.G.; Rucker, H.O.; Urpo, S. (2005). Low-frequency modulations in the solar microwave radiation as a possible indicator of inductive interaction of coronal magnetic loops. *Astronomy and Astrophysics*, Vol. 433, No. 2, 691–699, (DOI:10.1051/0004-6361:20041988).
- Khodachenko, M.L.; Rucker, H.O.; Kislyakov, A.G.; Zaitsev, V.V.; Urpo, S. (2006). Microwave Diagnostics of Dynamic Processes and Oscillations in Groups of Solar Coronal Magnetic Loops. *Space Science Reviews*, Vol. 122, No. 1-4, 137–148, (DOI:10.1007/s11214-006-7767-0).
- Khodachenko, M.L.; Zaitsev, V.V.; Kislyakov, A.G.; Stepanov, A.V. Equivalent Electric Circuit Models of Coronal Magnetic Loops and Related Oscillatory Phenomena on the Sun. (2009). *Space Science Reviews*, Vol. 149, No. 1-4, 83–117, (DOI:10.1007/s11214-009-9538-1).
- Khodachenko, M.L.; Kislyakova, K.; Zaqarashvili, T.V.; Kislyakov, A.G.; Panchenko, M.; Zaitsev, V.V.; Arkhypov, O.V.; Rucker, H.O. (2011). Possible manifestation of large-scale transverse oscillations of coronal loops in solar microwave emission. *Astronomy and Astrophysics*, Vol. 525, CiteID A105, (DOI:10.1051/0004-6361/201014860).
- Kislyakov, A. G.; Zaitsev, V. V.; Stepanov, A. V.; Urpo, S. (2006). On the Possible Connection between Photospheric 5-Min Oscillation and Solar Flare Microwave Emission. *Solar Physics*, Vol. 233, No. 1, 89–106, (DOI:10.1007/s11207-006-2850-y).
- Kislyakova, K.G.; Zaitsev, V.V.; Urpo, S.; Riehkainen, A. (2011). Long-period oscillations of the solar microwave emission. *Astronomy Reports*, Vol. 55, No. 3, 275–283, (DOI:10.1134/S1063772911030036).
- Kislyakov, A.G.; Shkelev, E.I.; Lupov, S.Y.; Kislyakova, K.G. (2011). Parameters of astrophysical objects according to their electromagnetic emission intensity modulation data. I. Observational data processing algorithms. *Bulletin of the Nizhny Novgorod State University*, No.2(1), 46–54, (in russian).

- LaRosa, T.N. & Moore, R.L. (1993). A Mechanism for Bulk Energization in the Impulsive Phase of Solar Flares: MHD Turbulent Cascade. *The Astrophysical Journal*, Vol. 418, 912–918, (DOI:10.1086/173448).
- Leka, K.D.; Canfield, R.C.; McClymont, A.N.; van Driel-Gesztelyi, L. (1996). Evidence for Current-carrying Emerging Flux. *The Astrophysical Journal*, Vol. 462, 547–560, (DOI:10.1086/177171).
- Marple, S. L., Jr. (1986). *Digital spectral analysis with applications*. Prentice-Hall, Inc. Upper Saddle River, NJ, USA, ISBN:0-132-14149-3.
- Miller, J.A.; LaRosa, T.N.; Moore, R.L. (1996). Stochastic Electron Acceleration by Cascading Fast Mode Waves in Impulsive Solar Flares. *The Astrophysical Journal*, Vol. 461, 445–464, (DOI:10.1086/177072).
- Miller, J.A.; Cargill, P.J.; Emslie, A.G.; Holman, G.D.; Dennis, B.R.; LaRosa, T.N.; Winglee, R.M.; Benka, S.G.; Tsuneta, S. (1997). Critical issues for understanding particle acceleration in impulsive solar flares. *Journal of Geophysical Research*, Vol. 102, No. A7, 14631–14660, (DOI:10.1029/97JA00976).
- Moreton, G.E. & Severny, A.B. (1968). Magnetic Fields and Flares in the Region CMP 20 September 1963. *Solar Physics*, Vol. 3, No. 2, 282–297, (DOI:10.1007/BF00155163).
- Nakariakov, V. M.; Foullon, C.; Verwichte, E.; Young, N. P. (2006). Quasi-periodic modulation of solar and stellar flaring emission by magnetohydrodynamic oscillations in a nearby loop. *Astronomy and Astrophysics*, Vol. 452, No. 1, 343–346, (DOI:10.1051/0004-6361:20054608).
- Panchenko, M.; Khodachenko, M. L.; Kislyakov, A. G.; Rucker, H. O.; Hanasz, J.; Kaiser, M. L.; Bale, S. D.; Lamy, L.; Cecconi, B.; Zarka, P.; Goetz, K. (2009). Daily variations of auroral kilometric radiation observed by STEREO, *Geophysical Research Letters*, Vol. 36, No. 6, CiteID L06102, (DOI:10.1029/2008GL037042).
- Pollock, D.S.G. (1999). *A handbook of time-series analysis, signal processing and dynamics*. London: Academic Press, ISBN:0-12-560990-6.
- Schrijver, C. J.; Title, A. M.; Berger, T. E.; Fletcher, L.; Hurlburt, N. E.; Nightingale, R. W.; Shine, R. A.; Tarbell, T. D.; Wolfson, J.; Golub, L.; Bookbinder, J. A.; Deluca, E. E.; McMullen, R. A.; Warren, H. P.; Kankelborg, C. C.; Handy, B. N.; de Pontieu, B. (1999). A new view of the solar outer atmosphere by the Transition Region and Coronal Explorer. *Solar Physics*, Vol. 187, No. 2, 261–302, (DOI:10.1023/A:1005194519642).
- Schrijver, C.J.; Aschwanden, M.J.; Title, A.M. (2002). Transverse oscillations in coronal loops observed with TRACE I. An Overview of Events, Movies, and a Discussion of Common Properties and Required Conditions. *Solar Physics*, Vol. 206, No. 1, 69–98, (DOI:10.1023/A:1014957715396).
- Schrijver, C.J. & Brown, D.S. (2000). Oscillations in the Magnetic Field of the Solar Corona in Response to Flares near the Photosphere. *The Astrophysical Journal*, Vol. 537, No. 1, L69–L72, (DOI:10.1086/312753).
- Shkelev, E.I.; Kislyakov, A.G.; Lupov, S.Y. (2002). Methods of decreasing of a cross-modulation effects in the Wigner-Ville distribution. *Izv. Vyss. Uchebn. Zaved., Ser. Radiofiz.* (transl. as *Radiophys. Quantum Electron.*), Vol. 45, No. 5, 433–442.
- Spangler, S.R. (2007). A Technique for Measuring Electrical Currents in the Solar Corona. *The Astrophysical Journal*, Vol. 670, No. 1, 841–848, (DOI:10.1086/521995).
- Tan, B.; Ji, H.; Huang, G.; Zhou, T.; Song, Q.; Huang, Y. (2006). Evolution of Electric Currents Associated with Two M-Class Flares. *Solar Physics*, Vol. 239, No. 1-2, 137–148, (DOI:10.1007/s11207-006-0120-7).

- Urpo, S.; Bakhareva, N.M.; Zaitsev, V.V.; Stepanov, A.V. (1994). Comparison of mm-wave and X-ray diagnostics of flare plasma. *Solar Physics*, Vol. 154, No. 2, 317–334, ISSN 0038-0938, (DOI:10.1007/BF00681102).
- Verwichte, E.; Foullon, C.; Van Doorselaere, T. (2010). Spatial Seismology of a Large Coronal Loop Arcade from TRACE and EIT Observations of its Transverse Oscillations. *The Astrophysical Journal*, Vol. 717, No. 1, 458–467, (DOI:10.1088/0004-637X/717/1/458).
- Ville, J. (1948). *Câbles et Transm.*, Vol. 2A, 61.
- Wigner, E. (1932). On the Quantum Correction For Thermodynamic Equilibrium. *Phys. Rev.*, Vol. 40, No. 5, 749–759, (DOI:10.1103/PhysRev.40.749).
- Zaitsev, V.V. & Stepanov, A.V. (1992). Towards the circuit theory of solar flares. *Solar Physics*, Vol. 139, No. 2, 343–356, ISSN 0038-0938, (DOI:10.1007/BF00159158).
- Zaitsev, V.V.; Stepanov, A.V.; Urpo, S.; Pohjolainen, S. (1998). LRC-circuit analog of current-carrying magnetic loop: diagnostics of electric parameters. *Astronomy and Astrophysics*, Vol. 337, 887–896.
- Zaitsev, V.V.; Kislyakov, A.G.; Urpo, S.; Shkelev E.I. (2001a). Observational evidence for energy accumulation and dissipation in coronal magnetic loops. *Izv. Vyssh. Uchebn. Zaved., Ser. Radiofiz.* (transl. as *Radiophys. & Quant. Electronics*), Vol. 44, No. 9, 697–709, (DOI:0033-8443/01/4409-0697\$25.00).
- Zaitsev, V.V.; Kislyakov, A.G.; Stepanov, A.V.; Urpo, S.; Shkelev E.I. (2001b). Low-frequency pulsations of coronal magnetic loops. *Izv. Vyssh. Uchebn. Zaved., Ser. Radiofiz.* (transl. as *Radiophys. & Quant. Electronics*), Vol. 44, No. 1-2, 36–52, (DOI:0033-8443/01/441-2-0036\$25.00).
- Zaitsev, V.V.; Kislyakov, A.G.; Urpo, S.; Stepanov, A.V.; Shkelev E.I. (2003). Spectral-Temporal Evolution of Low-Frequency Pulsations in the Microwave Radiation of Solar Flares. *Astronomy Reports*, Vol. 47, No. 10, 873–882, (DOI:10.1134/1.1618999).
- Zaitsev, V.V.; Kislyakov, A.G.; Stepanov, A.V.; Kliem, B.; Fürst, E. (2004). Pulsating Microwave Emission from the Star AD Leo. *Astronomy Letters*, Vol. 30, 319–324, (DOI:10.1134/1.1738154).
- Zaitsev, V. V.; Kislyakov, A. G.; Kislyakova, K. G. (2008). Parametric resonance in the solar corona. *Cosmic Research*, Vol. 46, No. 4, 301–308, (DOI:10.1134/S0010952508040035).
- Zaitsev, V. V. & Kislyakov, A. G. (2006). Parametric excitation of acoustic oscillations in closed coronal magnetic loops. *Astronomy Reports*, Vol. 50, No. 10, 823–833, (DOI:10.1134/S1063772906100076).



Fourier Transform Applications

Edited by Dr Salih Salih

ISBN 978-953-51-0518-3

Hard cover, 300 pages

Publisher InTech

Published online 25, April, 2012

Published in print edition April, 2012

The book focuses on Fourier transform applications in electromagnetic field and microwave, medical applications, error control coding, methods for option pricing, and Helbert transform application. It is hoped that this book will provide the background, reference and incentive to encourage further research and results in these fields as well as provide tools for practical applications. It provides an applications-oriented analysis written primarily for electrical engineers, control engineers, signal processing engineers, medical researchers, and the academic researchers. In addition the graduate students will also find it useful as a reference for their research activities.

How to reference

In order to correctly reference this scholarly work, feel free to copy and paste the following:

Maxim L. Khodachenko, Albert G. Kislyakov and Eugeny I. Shkelev (2012). Analysis of Long-Periodic Fluctuations of Solar Microwave Radiation, as a Way for Diagnostics of Coronal Magnetic Loops Dynamics, Fourier Transform Applications, Dr Salih Salih (Ed.), ISBN: 978-953-51-0518-3, InTech, Available from: <http://www.intechopen.com/books/fourier-transform-applications/analysis-of-long-periodic-fluctuations-of-solar-microwave-radiation-as-a-way-for-diagnostics-of-coro>

INTECH
open science | open minds

InTech Europe

University Campus STeP Ri
Slavka Krautzeka 83/A
51000 Rijeka, Croatia
Phone: +385 (51) 770 447
Fax: +385 (51) 686 166
www.intechopen.com

InTech China

Unit 405, Office Block, Hotel Equatorial Shanghai
No.65, Yan An Road (West), Shanghai, 200040, China
中国上海市延安西路65号上海国际贵都大饭店办公楼405单元
Phone: +86-21-62489820
Fax: +86-21-62489821

© 2012 The Author(s). Licensee IntechOpen. This is an open access article distributed under the terms of the [Creative Commons Attribution 3.0 License](#), which permits unrestricted use, distribution, and reproduction in any medium, provided the original work is properly cited.

IntechOpen

IntechOpen